Water Driven *Cu* Nanoparticles between two Concentric ducts with Oscillatory Pressure Gradient

Faisal Shahzad [1], *Rizwan Ul Haq*[2,*], *Qasem M. Al-Mdallal*[3]

[1]*Department of Mathematics, Capital University of Science and Technology, Islamabad 44000, Pakistan*

[2]*Department of Computer Science, Bahria University, Islamabad Campus, Islamabad, 44000, Pakistan*

[3]*Department of Mathematical Sciences, UAE University, Al Ain, P.O. Box 15551, UAE*

Abstract

Current study is devoted to examine the magneto-hydrodynamics (MHD) flow of water based Cu Nanoparticles with oscillatory pressure gradient between two concentric cylinders. Arrived broad, it is perceived that the inclusion of nanoparticles has increased considerably the heat transfer near the surface of both laminar and turbulent regimes. Mathematical model is constructed in the form of partial differential equations which contains the effective thermal conductivity and viscosity of base fluid and nanoparticles. Close form solution is attained corresponding to the momentum and energy equation and results are evaluated for velocity, temperature and pressure gradient in the restricted domain. Graphical results for numerical values of the flow control parameters: Hartmann number M, Reynolds number Re_ω, the solid volume fraction of nanoparticles ϕ and the pulsation parameter based on the periodic pressure gradient have been presented for the pressure difference, frictional forces, velocity profile, temperature profile, and vorticity phenomena have been discussed. The assets of various parameters on the flow quantities of observation are investigated. To the same degree a concluding crux, the streamlines are examined and plotted. The results confirmed that the velocity and temperature may be controlled with the aid of the outside magnetic field and due to the growth in the nanoparticles and considerable enhancement in the heat transfer rate can be found by adding/removing the strength of magnetic field and nanoparticle volume fraction.

Keywords: MHD, Pulsating flow, H_2O, nanofluid, MHD, concentric cylinders

[*] *Corresponding author: R. U. Haq (ideal_riz@hotmail.com, r.haq.qau@gmail.com), Phone No. +92 3335371853*

1. Introduction

Flow through a cylindrical shape is one of the most important and fundamental natural process at industrial level. Apart from industry, this fundamental process also used in daily life problems like; distribution of water in house from water through a cylindrical shape pipe, heart pumping and distribution of blood in all parts of body through cylindrical shape blood vessels, in ideal fluid like gas which is use for burning is also distributed through cylindrical iron pipes and also preserved in cylinders. The main question is why most often we use cylindrical shapes for all these process. There are several matters of fact but foremost important factor is to reduce the drag force with the surface so the fluid can travel faster in cylindrical shape duct as compare to others shapes. Sometime flow cannot be generated unless an external force will apply. There is several ways to drive the fluid in cylinder but pressure is the most appropriate way to enhance the tendency of fluid motion. The phenomenon that deals the flow through a cylinder shape via pressure is known as pulsatile flow. The flow through cylinder with oscillatory motion have many significant applications in real life like; blood flow through an artery, motion of urine in urethra, peristaltic food motion in the intestine.

Basic concept and analytical solution is constructed for velocity for time dependent flow in cylindrical shape pipe is presented by Atabek et al. [1]. In another study, Vardanyan et al. [2] construct many interesting and theoretical prototypes to discover the impact of MHD on flow through cylindrical pipes. Likewise, Chaturani and Palanisamy [3] present the impact of oscillatory body acceleration on blood motion due to pulsatile flow. They have determined the analytical solution of pulsatile flow of blood via finite Hankel and Laplace transforms. It is worth worthy to note that increase in the axial velocity provide the transformation of fluid momentum from axis of tube and the nearest region of tube wall with respect to increase in the diameter of tube. In the recent decay, Moustafa El-Shahed [4] extended the idea of Chaturani and Palanisamy [3] and attained the analytical results via Laplace and Hankel transform for pulsatile motion of blood flow through a porous medium with same oscillatory body force. He has found that velocity profile is increasing function of permeable parameter and provides the comparison for limiting case of his model. In recent study Mathur and Jain [5], discussed the concept blood flow through stenosed tube with oscillatory body force with magnetic field strength. Again these results are obtained through Hankel and Laplace transforms in term of Bessel–Fourier series form. The

significant influence of magnetic field is also obtained in this study. Sankar and Hemalatha [6] discussed the pulsatile flow in a catheterized artery. In this model non-Newtonian Herschel-Bulkely fluid has been presented for two parameters namely: yield stress and power index. Dulal Chandra Sanyal and Ananda Biswas [7] have proven under the normal conditions, blood go with the flow inside the human circulatory system relies and it depends upon the pumping of coronary heart and this phenomena is due to the pressure gradient within the entire body. In another study, Yakhot et al. [8] discover the impact of rate of pressure and difference of phase on the velocity profile. Suces et al. [9] successfully attain the numerical result for reaction features near the temperature of the wall and the average temperature between a laminar drift to the flat plate by mean of finite difference technique (FDM). Later on many researchers have discussed the phenomena of channel flow with various conditions on pressure [10-14].

Nanofluid is just a fluid comprising nanometer-sized particles, referred to as nanoparticles. Using nanofluids is to improve the heat-switch overall performance of the working fluids due to the fact they on the entire work as a coolant with a heat transfer device. Initially, main concept of nanofluid is conceived by Choi [15]. Nanofluid contains important thermosphysical properties such as thermal conductivity, thermal diffusivity, viscosity and convective heat transfer coefficients comparable to other Newtonian and non-Newtonian fluids like oil or water [16-19]. Important slip mechanism is presented by Buongiorno [20], in which he has presented the heat efficiency by visualizing the contribution of both Brownian motion and thermophoresis of nanoparticles. In another study, Akbar et al. [21] analyze the viscoelastic fluid models in the presence of nanoparticles with magnetic strength for mixed convection flow. Recently, Ebaid et al. [22, 23] thoroughly discussed the results for nanofluid in boundary layer regime. Close form solutions are determined to acquire the velocity and temperature by variating the values of emerging parameters. Recently, many authors have discussed the nanofluid flow phenomena for various types of working fluids and nanoparticle for different geometries [24-40].

Main emphasis of the problem is to describe the fluid based totally at the mathematical version of the Cu nanofluid with H_2O as a liquid. In biomedicine copper particles play an important role by showing their significant use in drug delivery at various parts of human body like: to vanishing tumor, heart rhythms, arthritis, thyroid glands, and wound recovery. Red blood cells formation and cholesterol are different health advantages of Cu. In fact human body has complex homeostatic mechanisms which try to make certain a regular deliver of available

copper, whilst doing away with extra copper whenever this happens. Standards followed via some countries advise special copper intake ranges for adults, girls, toddlers, and kids, similar to the varying wishes for copper throughout one of kind ranges of life. The conventional governing equations based upon fundamental momentum and energy equations are formulated and then problem is solved analytically to achieve the precise answers within the shape of Bessel function. The obtained expressions for velocity, temperature and pressure gradient are discussed graphically through variant in bodily parameters.

Nomenclature

ρ_{nf}	Density of nanofluid	M	Hartmann number
μ_{nf}	Viscosity of nanofluid	Pr	Prandtl number
C_{nf}	Specific heat of nanofluid	Re_{ω}	Reynolds number
k_{nf}	Thermal conductivity of nanofluid	t	Time
σ_{nf}	Electric conductivity of nanofluid	D	Diameter
ρ_f	Density of fluid	r	Radius
ρ_p	Density of nanoparticles	T	Temperature
C_f	Specific heat of the fluid	u,v,w	Velocity components
C_p	Specific heat of the nanoparticles	$\vec{J}$	Current density
σ_f	Eelectric conductivity of the fluid	$\vec{B}$	Magnetic field
σ_p	Electric conductivity of the nanoparticles	H	Magnetic field intensity
k_f	Thermal conductivity of the fluid	C	Velocity of light
k_p	Thermal conductivity of the nano particles	L	Length of the cylinder
μ_f	Dynamic viscosity of the fluid	ϕ	Volume fraction of the nanoparticles
μ_p	Dynamic viscosity of nanoparticles	R^*=Ri/Re	
α	Womersley Number ($=\sqrt{Re_{\omega}}$)	**Used Indexes**	
γ	Temperature gradient	i	Internal
A	Amplitude	e	External
ω	Pulsation	f	Fluid
P	Pressure	p	Particle

3. Mathematical formulation

2.1 Physical problem

A unidirectional Magneto-hydrodynamic flow of a viscous fluid passed through two equally concentric cylinders is established in a cylindrical coordinate system (*rz*-planar) according to the constrained shown in Fig. 1. To boost the thermal conductivity of working fluid we have saturated the Copper nanoparticles (*Cu*) within the water. To drive the fluid within the defined channel we have applied oscillatory pressure gradient in longitudinal direction (*z*-direction). Since flow is due to pressure gradient therefor velocity of the walls of the cylinders is zero. However, the temperature of the external duct is adiabatic and uniform (400 Kelvin) at the internal duct. It is further assumed that atmospheric pressure and temperature is about 300 Kelvin.

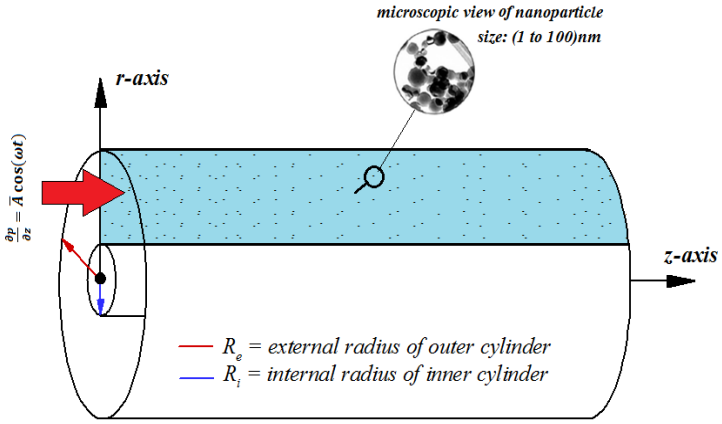

Fig. 1 Flow field geometry.

2.2 Governing equations

Assumptions

As we have considered the fluid is incompressible, viscous and electrically conducting so we have constructed the mathematical model that is based upon conventional continuity, momentum and energy equations:

$$\nabla \cdot \vec{V} = 0 \tag{1}$$

$$\rho_{nf}\left(\frac{\partial \vec{V}}{\partial t} + \vec{V}.\nabla\vec{V}\right) = -\nabla P + \mu_{nf}\nabla^2\vec{V} + \left(\vec{J} \times \vec{B}\right).\vec{V} \tag{2}$$

$$(\rho C)_{nf}\left(\frac{\partial T_f}{\partial t}+\left(\vec{V}.\nabla T_f\right)\right)=K_{nf}\nabla^2 T \tag{3}$$

In cylindrical coordinates system, equation of continuity, momentum and energy are given to be:

$$\frac{\partial u}{\partial r}+\frac{\partial w}{\partial z}+\frac{u}{r}=0, \tag{4}$$

$$\rho_{nf}\left(\frac{\partial u}{\partial t}+u\frac{\partial u}{\partial r}+w\frac{\partial u}{\partial z}\right)=-\frac{\partial P}{\partial r}+\mu_{nf}\left[\frac{\partial^2 u}{\partial r^2}+\frac{1}{r}\frac{\partial u}{\partial r}+\frac{\partial^2 u}{\partial z^2}-\frac{u}{r^2}\right], \tag{5}$$

$$\rho_{nf}\left(\frac{\partial w}{\partial t}+u\frac{\partial w}{\partial r}+w\frac{\partial w}{\partial z}\right)=-\frac{\partial P}{\partial z}+\mu_{nf}\left[\frac{\partial^2 w}{\partial r^2}+\frac{1}{r}\frac{\partial w}{\partial r}+\frac{\partial^2 w}{\partial z^2}\right]-\sigma_{nf}B_o^2 w, \tag{6}$$

$$(\rho C)_{nf}\left(\frac{\partial T}{\partial t}+u\frac{\partial T}{\partial r}+w\frac{\partial T}{\partial z}\right)=K_{nf}\left[\frac{\partial^2 T}{\partial r^2}+\frac{1}{r}\frac{\partial T}{\partial r}+\frac{\partial^2 T}{\partial z^2}\right]. \tag{7}$$

where, ρ_{nf}, μ_{nf}, $(\rho C)_{nf}$, k_{nf} and σ_{nf} are the density, dynamic viscosity, specific heat, thermal conductivity and electric conductivity of nanofluid, respectively. These expression are defined as:

$$\mu_{nf}=\frac{\mu_f}{(1-\phi)^{2.5}}, \tag{8a}$$

$$(\rho C)_{nf}=(1-\phi)(\rho C)_f+\phi(\rho C)_p, \tag{8b}$$

$$\rho_{nf}=(1-\phi)\rho_f+\phi\rho_p, \tag{8c}$$

$$\frac{k_{nf}}{k_f}=\frac{k_p+2k_f-2\phi(k_f-k_p)}{k_p+2k_f+\phi(k_f-k_p)}, \tag{8d}$$

$$\frac{\sigma_{nf}}{\sigma_f}=1+\frac{3\left(\frac{\sigma_p}{\sigma_f}-1\right)\phi}{\left(\frac{\sigma_p}{\sigma_f}+2\right)-\left(\frac{\sigma_p}{\sigma_f}-1\right)\phi}. \tag{8e}$$

The expression of effective thermal conductivity k_{nf}/k_f is introduced by Hamilton and Crosser [40]. This model depends upon the empirical shape factor n for the nanoparticle. In particular, $n=3$ for spherical shaped nanoparticles and $n=3/2$ for cylindrical ones. In view of above mentioned quantities, equations (5)-(7) take the following forms, respectively:

$$\left((1-\phi)\rho_f+\phi\rho_p\right)\left(\frac{\partial u}{\partial t}+u\frac{\partial u}{\partial r}+w\frac{\partial u}{\partial z}\right)=-\frac{\partial P}{\partial r}+\frac{\mu_f}{(1-\phi)^{2.5}}\left[\frac{\partial^2 u}{\partial r^2}+\frac{1}{r}\frac{\partial u}{\partial r}+\frac{\partial^2 u}{\partial z^2}-\frac{u}{r^2}\right], \tag{9a}$$

$$\left((1-\phi)\rho_f + \phi\rho_p\right)\left(\frac{\partial w}{\partial t} + u\frac{\partial w}{\partial r} + w\frac{\partial w}{\partial z}\right) = -\frac{\partial P}{\partial z} + \frac{\mu_f}{(1-\phi)^{2.5}}\left[\frac{\partial^2 w}{\partial r^2} + \frac{1}{r}\frac{\partial w}{\partial r} + \frac{\partial^2 w}{\partial z^2}\right] - \sigma_{nf}B_o^2 w, \quad (9b)$$

$$\left((1-\phi)(\rho C)_f + \phi(\rho C)_p\right)\left(\frac{\partial T}{\partial t} + u\frac{\partial T}{\partial r} + w\frac{\partial T}{\partial z}\right) = K_{nf}\left[\frac{\partial^2 T}{\partial r^2} + \frac{1}{r}\frac{\partial T}{\partial r} + \frac{\partial^2 T}{\partial z^2}\right]. \quad (9c)$$

The system can be expressed in dimensionless terms by defining the following quantities:

$u = \frac{u'}{\omega R_e}, w = \frac{w'}{\omega R_e},\ r = \frac{\acute{r}}{R_e}, z = \frac{\acute{z}}{R_e},\ t = \omega t', T = \frac{T\prime - T_f}{T_i - T_f}, P = \frac{P\prime}{\rho_f R_e^2 \omega^2}, \nu_f = \frac{\mu_f}{\rho_f}, Re_\omega = \alpha^2 = \frac{\omega R_e^2}{\nu_f}, Pr = \frac{\mu_f C_f}{k_f}, M = R_e B_o\sqrt{\frac{\sigma_f}{\mu_f}}$.

In the above expression $Re_\omega = \frac{\omega R_e^2}{\nu_f}$ is Reynolds number, $\mathrm{Pr} = \frac{\mu_f C_f}{k_f}$ Prandtl number and $M = RB_o\sqrt{\frac{\sigma_f}{\mu_f}}$ Hartmann number. Dimensionless form of the equations (9a) to (9c) is given by:

$$A_1\left(\frac{\partial u}{\partial t} + u\frac{\partial u}{\partial r} + w\frac{\partial u}{\partial z}\right) = -\frac{\partial P}{\partial r} + \frac{1}{(1-\phi)^{2.5}Re_\omega}\left[\frac{\partial^2 u}{\partial r^2} + \frac{1}{r}\frac{\partial u}{\partial r} + \frac{\partial^2 u}{\partial z^2} - \frac{u}{r^2}\right], \quad (10a)$$

$$A_1\left(\frac{\partial w}{\partial t} + u\frac{\partial w}{\partial r} + w\frac{\partial w}{\partial z}\right) = -\frac{\partial P}{\partial z} + \frac{1}{(1-\phi)^{2.5}Re_\omega}\left[\frac{\partial^2 w}{\partial r^2} + \frac{1}{r}\frac{\partial w}{\partial r} + \frac{\partial^2 w}{\partial z^2}\right] - A_2\frac{M^2 w}{Re_\omega}, \quad (10b)$$

$$A_3\left(\frac{\partial T}{\partial t} + u\frac{\partial T}{\partial r} + w\frac{\partial T}{\partial z}\right) = \frac{A_4}{PrRe_\omega}\left[\frac{\partial^2 T}{\partial r^2} + \frac{1}{r}\frac{\partial T}{\partial r} + \frac{\partial^2 T}{\partial z^2}\right]. \quad (10c)$$

Hhere, the coefficients A_1, A_2, A_3 and A_4 are defined as:

$$\left.\begin{aligned} A_1 &= (1-\phi) + \phi\frac{\rho_p}{\rho_f}, \\ A_2 &= \frac{\sigma_{nf}}{\sigma_f} = 1 + \frac{3\left(\frac{\sigma_p}{\sigma_f} - 1\right)\phi}{\left(\frac{\sigma_p}{\sigma_f} + 2\right) - \left(\frac{\sigma_p}{\sigma_f} - 1\right)\phi}, \\ A_3 &= (1-\phi) + \phi\frac{(\rho C)_p}{(\rho C)_f}, \\ A_4 &= \frac{K_{nf}}{K_f} = \frac{k_p + 2k_f - 2\phi(k_f - k_p)}{k_p + 2k_f + \phi(k_f - k_p)}. \end{aligned}\right\} \quad (11)$$

2.3 Boundary Conditions

The associated initial and boundary conditions of the model will take the following forms:

At $t = 0$

$$u(r,z,0) = w(r,z,0) = 0 \quad \text{and} \quad p(r,z,0) = T_f(r,z,0) = 0. \quad (12a)$$

For external duct

$$u(1,z,t) = w(1,z,t) = 0 \quad \text{and} \quad \frac{\partial T_f}{\partial r}(1,z,t) = 0. \tag{12b}$$

For internal duct

$$u\left(\frac{R_i}{R_e},z,t\right) = w\left(\frac{R_i}{R_e},z,t\right) = 0 \text{ and } T_f\left(\frac{R_i}{R_e},z,t\right) = 1. \tag{12b}$$

In order to find the close form solution, we expect that model is fully developed and the velocity field is described as:

$$\vec{V} = [0,0,w(r,z,t)]. \tag{13}$$

The fluid flow governing equations could be rewritten in the form,

$$A_1 \frac{\partial w}{\partial t} = -\frac{\partial P}{\partial z} + \frac{1}{(1-\phi)^{2.5} Re_\omega}\left[\frac{\partial^2 w}{\partial r^2} + \frac{1}{r}\frac{\partial w}{\partial r}\right] - A_2 \frac{M^2 w}{Re_\omega}, \tag{14a}$$

$$A_3\left(\frac{\partial T}{\partial t} + w\frac{\partial T}{\partial z}\right) = \frac{A_4}{\mathrm{Pr} Re_\omega}\left[\frac{\partial^2 T}{\partial r^2} + \frac{1}{r}\frac{\partial T}{\partial r} + \frac{\partial^2 T}{\partial z^2}\right]. \tag{14b}$$

The dimensionless form of equations 14(a) and 14(b) implies:

$$A_1 \frac{\partial w}{\partial t} = -\frac{\partial P}{\partial z} + \frac{A_5}{\alpha^2}\left[\frac{\partial^2 w}{\partial r^2} + \frac{1}{r}\frac{\partial w}{\partial r}\right] - A_2 \frac{M^2 w}{\alpha^2}, \tag{15a}$$

$$A_3\left(\frac{\partial T}{\partial t} + w\frac{\partial T}{\partial z}\right) = \frac{A_4}{\mathrm{Pr}\alpha^2}\left[\frac{\partial^2 T}{\partial r^2} + \frac{1}{r}\frac{\partial T}{\partial r} + \frac{\partial^2 T}{\partial z^2}\right], \tag{15b}$$

where, $A_5 = \frac{1}{(1-\phi)^{2.5}}$.

2.4 Solution of the problem

Since the present phenomena deals with the study of pulsatile flow, therefore pressure gradient could be expressed in the form,

$$\frac{\partial P}{\partial z} = -\bar{A}Cos(\omega t) = \mathrm{Re}\left(-\bar{A}e^{i\omega t}\right). \tag{16}$$

The supposed form of the solution for velocity profile can be defined as

$$w(r,t) = \mathrm{Real}\left(f(r)e^{i\omega t}\right) \tag{17}$$

In view of above equations, we have from equation (15a)

$$\frac{d^2f(r)}{dr^2}+\frac{1}{r}\frac{df(r)}{dr}-\frac{1}{A_5}(M^2A_2+i\alpha^2A_1)f(r)=-\frac{1}{A_5}\mathrm{A}\alpha^2 \tag{18}$$

The solution obtained from equation (18) is in the shape of Bessel function, i.e.

$$f(r)=C_1I_0(\eta r)+C_2K_0(\eta r), \tag{19}$$

where I_0 Bessel functions of first kind and K_0 are Bessel functions second kind and $\eta=\sqrt{M^2A_2+i\alpha^2A_1}$. To be able to determine C_1 and C_2, we use the boundary conditions

$$r=\frac{R_i}{R_e}=R^*, r=1 \quad w=0. \tag{20}$$

From equation (17), the velocity solution profile can be indicted as

$$w(r,t)=Real\left[C_1I_0(\eta r)+C_2K_0(\eta r)+\frac{A\alpha^2}{A_5\eta^2}\right]e^{it}, \tag{21}$$

Where the constants C_1 and C_2 are defined as:

$$C_1=-\frac{\alpha^2BesselK[0,\eta]\bar{A}-\alpha^2BesselK[0,\eta R^*]\bar{A}}{\eta^2(BesselI[0,\eta R^*]BesselK[0,\eta]-BesselI[0,\eta]BesselK[0,\eta R^*])A_5}$$

and $$C_2=-\frac{-\alpha^2BesselI[0,\eta]\bar{A}+\alpha^2BesselI[0,\eta R^*]\bar{A}}{\eta^2(BesselI[0,\eta R^*]BesselK[0,\eta]-BesselI[0,\eta]BesselK[0,\eta R^*])A_5}.$$

Again from equation (15b), it is assume that solution of temperature profile is defined as:

$$T(r,z,t)=Real[-\gamma^*z+\gamma^*\,g(r)\,e^{it}+1]. \tag{22}$$

Where $\gamma^*=\frac{Re}{L}$ and equation (15b) will give us:

$$\frac{d^2g(r)}{dr^2}+\frac{1}{r}\frac{dg(r)}{dr}-i\frac{A_3\alpha^2Pr}{A_4}g(r)=\frac{A_3\alpha^2Pr}{A_4}f(r). \tag{23}$$

Using the boundary conditions,

$$r=R^* \implies T=1 \text{ and } r=1 \implies \frac{\partial T}{\partial r}=0. \tag{24}$$

Solution of temperature profile can also written as:

$$T(r,z,t)=Real[-\gamma^*z+\gamma^*[-iC_1I_0(\eta r)-iC_2K_0(\eta r)+C_3I_0(\xi r)$$

$$+C_4K_0(\xi r) - \frac{iA\alpha^2}{\eta^2}]e^{it} + 1] \tag{25}$$

where $\xi = \alpha\sqrt{\frac{i\mathrm{Pr}A_3}{A_4}}$,

$$C_3 = \frac{\alpha\eta^2\sqrt{\mathrm{iPr}}\sqrt{A_3}A_5\mathrm{BesselK}[1,\xi]\delta_1 + \eta^3\sqrt{A_4}A_5\mathrm{BesselK}[0,\xi R^*]\delta_2}{\alpha\eta^2\sqrt{\mathrm{iPr}}(\mathrm{BesselI}[1,\xi]\mathrm{BesselK}[0,\xi R^*] + \mathrm{BesselI}[0,\xi R^*]\mathrm{BesselK}[1,\xi])},$$

$$C_4 = \frac{\alpha\eta^2\sqrt{\mathrm{iPr}}\sqrt{A_3}A_5\mathrm{BesselI}[1,\xi]\delta_1 - \eta^3\sqrt{A_4}A_5\mathrm{BesselI}[0,\xi R^*]\delta_2}{\alpha\eta^2\sqrt{\mathrm{iPr}}(\mathrm{BesselI}[1,\xi]\mathrm{BesselK}[0,\xi R^*] + \mathrm{BesselI}[0,\xi R^*]\mathrm{BesselK}[1,\xi])},$$

$$\delta_1 = i\left[\mathrm{BesselI}[0,\eta R^*]C_1 + \mathrm{BesselK}[0,\eta R^*]C_2 + \frac{\alpha^2}{A_5\eta^2}\bar{A} - i\frac{z}{e^{\mathrm{it}}}\right],$$

$$\delta_2 = i[\mathrm{BesselI}[1,\eta]C_1 - \mathrm{BesselK}[1,\eta]C_2].$$

2.5 Pressure calculation

From equation (15a) we have

$$\frac{\partial P}{\partial z} = -A_1\frac{\partial w}{\partial t} + \frac{A_5}{\alpha^2}\left[\frac{\partial^2 w}{\partial r^2} + \frac{1}{r}\frac{\partial w}{\partial r}\right] - A_2\frac{M^2 w}{\alpha^2}. \tag{26}$$

Substituting the solution obtained for $w(r,t)$ in equation (26)

$$\frac{\partial P}{\partial z} =$$
$$-A_1(ie^{it}(\frac{\alpha^2\bar{A}}{\eta^2A_5^2} + \frac{Bessel\ I[0,r\eta]c_1}{\eta^2A_5^2} - \frac{Bessel\ K[0,r\eta]c_2}{\eta^2A_5^2}) + \frac{\alpha^2\bar{A}}{({A_5}^2\eta^2)})e^{it}) +$$
$$\frac{A_5}{\alpha^2}(e^{it}(\frac{(Bessel\ I[0,r\eta]+Bessel\ I[2,r\eta])c_1}{2A_5^2} + \frac{(-Bessel\ K[0,r\eta]-Bessel\ K[2,r\eta])c_2}{2A_5^2}) + \frac{1}{r}e^{it}(\frac{Bessel\ I[1,r\eta]c_1}{\eta A_5^2} +$$
$$\frac{BesselK[1,r\eta]c_2}{\eta A_5^2}))c_2 - \frac{A_2M^2}{\alpha^2}(BesselI[0,r\times\eta]\frac{1}{({A_5}^2\eta^2)}c_1 - BesselK[0,r\times\eta]\frac{1}{({A_5}^2\eta^2)}). \tag{27}$$

The dimensionless pressure rise is define as

$$\Delta P = \int_0^1 \frac{\partial P}{\partial z}dz \tag{28}$$

$$\Delta P = -A_1\left(ie^{it}\left(\frac{\alpha^2\bar{A}}{\eta^2 A_5^2} + \frac{\text{BesselI}[0,r\eta]c_1}{\eta^2 A_5^2} - \frac{\text{BesselK}[0,r\eta]c_2}{\eta^2 A_5^2}\right) + \frac{\alpha^2\bar{A}}{({A_5}^2\eta^2)}\right)e^{it}) + \frac{A_5}{\alpha^2}\left(e^{it}\left(\frac{(\text{BesselI}[0,r\eta]+\text{BesselI}[2,r\eta])c_1}{2A_5^2} + \frac{(-\text{BesselK}[0,r\eta]-\text{BesselK}[2,r\eta])c_2}{2A_5^2}\right) + \frac{1}{r}e^{it}\left(\frac{\text{BesselI}[1,r\eta]c_1}{\eta A_5^2} + \frac{\text{BesselK}[1,r\eta]c_2}{\eta A_5^2}\right)\right)c_2 - \frac{A_2 M^2}{\alpha^2}\left((\text{BesselI}[0, r\times\eta] * \frac{1}{({A_5}^2\eta^2)}c_1 - \text{BesselK}[0, r\times\eta]\frac{1}{({A_5}^2\eta^2)}\right). \quad (29)$$

Expression for stream function is given as follows:

$$w(r,t) = \frac{1}{r}\frac{\partial\psi}{\partial r}. \quad (30)$$

Table 1: Thermo-physical properties of H_2O Based Cu.

Phase	ρ (Kg/m^3)	k (W/mK)	C (J/kg K)	σ (s/m)
H_2O (Water)	997.1	0.613	4179	0.05
Cu(Copper)	8933	400	385	5.96×10^7

4. Results and Discussion

In order to obtain an insight into the physics of the problem, computations of velocity profile, temperature profile, vorticity, pressure rise, and streamlines are plotted for various values of magnetic field parameter M, kinetic Reynolds number Re_ω, nanoparticle volume fraction ϕ, amplitude of pressure gradient $\bar{A}$, Prandtl number Pr and time t.

The axial velocities are studied which varies from inlet to outlet and affect the heat transfer rate in particular region due to development of flow. For one complete pulsation cycle of 360° the instances were taken at each $t = 30^\circ$ to calculate the axial velocity variation at particular volume fraction ϕ. All the captured instances are in total 12 for a complete cycle of 360°. Figures 2(a) and 2(b) are ready to study the impact of various values of nanoparticle volume fraction at velocity distribution. Each plotted figure represents that the velocity profile traces a parabolic trajectory and attain maximum distribution of velocity at the mean position of the channel and rapidly decreases with rise of volume fraction. It is also illustrated from Figures 2(a) and 2(b) that inclusion of nanoparticles provides the increase of density of whole mixture. In figure 2(a), one can observe that there is a significant and higher disturbance in the velocity

profile for base fluid (ϕ=0) as compare to the nonzero values of nanoparticle volume fraction. Physically, we can say that by incorporating the nanoparticles within the water then the density of whole mixture will increase considerably. Consequently, when density of nanofluid increases then motion of nanofluid become slow as compare to the base fluid (water) as shown in Figs. 2(a) and 2(b). Figures 3(a) and 3(b) illustrate that velocity maximum are found at the vicinity of the cylinder's walls with rapid vibrations due to annular effect. These annular effects rise due to Womersley number Re_ω.

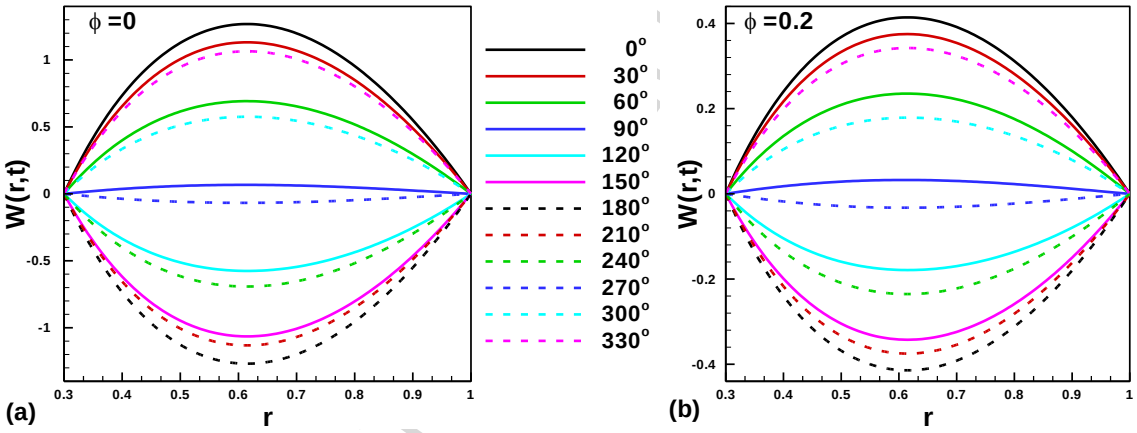

Fig. 2: Variation of velocity profile when $M = 0, Re_\omega = 1$ **(a)** $\phi = 0$ **(b)** $\phi = 0.2$.

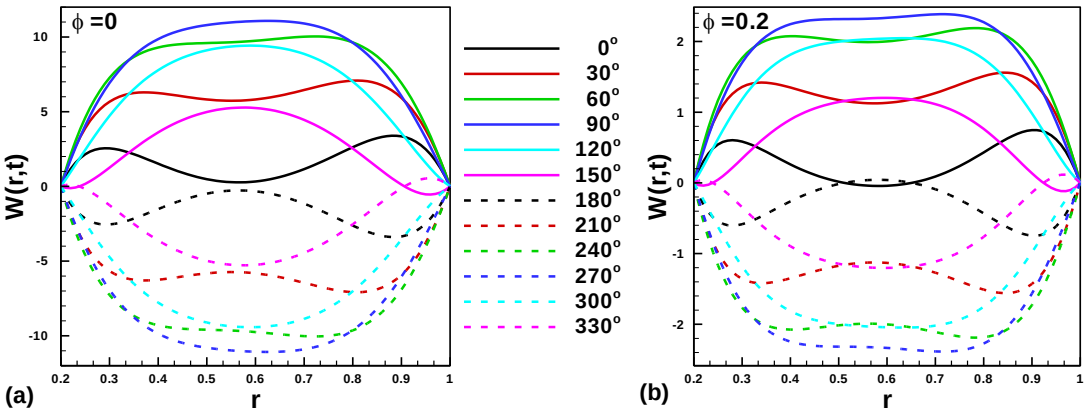

Fig. 3. Variation of velocity profile when $M = 0, Re_\omega = 10$ **(a)** $\phi = 0$ **(b)** $\phi = 0.2$.

It is shown that with increase of Re_w velocity slightly deviate from sinusoidal mean velocity for certain instance of time. With increase of Re_w gives rise to the more substantial annular effect and in this way the radial velocity nearby cylinder wall become steeper and friction force

increases with increase of Re_w. Inertial components increase in momentum equation with increase of Re_ω. Further it is notice that by increase of Womersley number provides the increase of velocity profile. Since, Womersley number is the ratio of pulsation to the viscous forces and when we increase the Womersley number then viscous forces will reduce. When viscous forces will then reduce then motion of the fluid particles become faster and consequently velocity profile will increase gradually (see Fig. 4(a) and 4(d)). Figure 5 is plotted in the comparison of Fig. 4 for Hartmann number. In Fig. 4, we have found that velocity distribution is adjacent along the walls of the ducts for M=0. However, for M=10 velocity distribution attains maximum amplitude at the mean position and trace the parabolic trajectory (See Fig. 5). It can further compare from Fig. 4 and Fig. 5 that increase in Hartmann number pretend provides squeeze the amplitude of velocity profile due to restive force. It is also obtained from Figures 5(a) and 5(b) that by the addition of nanoparticles lessens the maximum velocity of the base fluid. It could be comprehended from Figs. 5, 6 (a) and 6(b) that the magnetic field serves as a retardant towards the flow, which ends up decrease the flow rate. Furthermore, the magnetic field gives rise to eliminate the annular effect that is considered as a feature of the pulsatile flow.

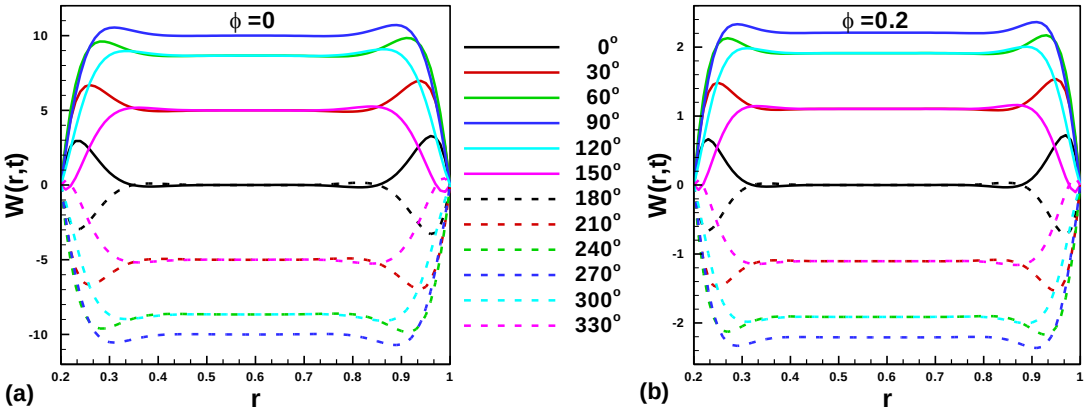

Fig. 4: Variation of velocity profile when $M = 0$, $Re_\omega = 30$ **(a)** $\phi = 0$ **(b)** $\phi = 0.2$.

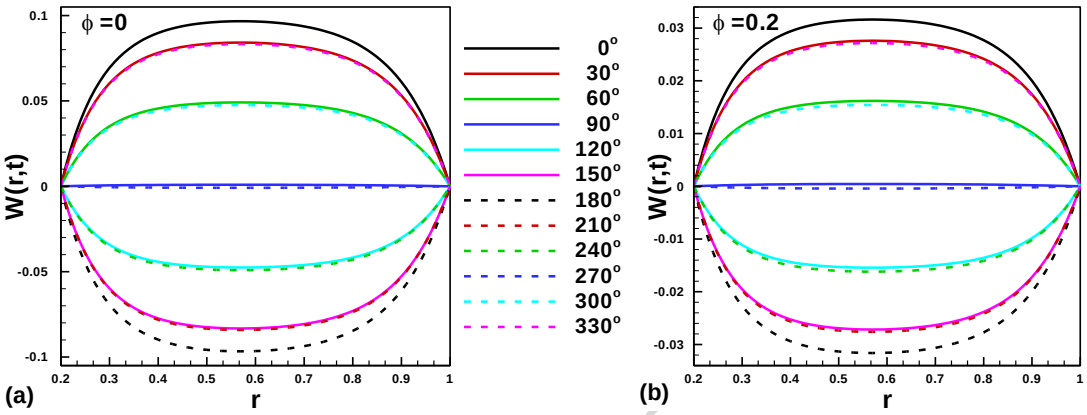

Fig. 5: Variation of velocity profile when $M = 10, Re_{\omega} = 1$ **(a)** $\phi = 0$ **(b)** $\phi = 0.2$.

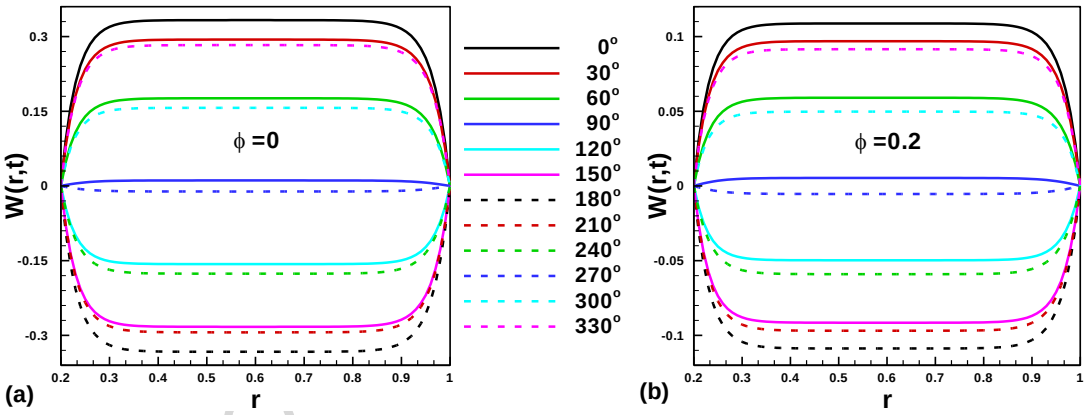

Fig. 6: Variation of velocity profile when $M = 30, Re_{\omega} = 30$ **(a)** $\phi = 0$ and **(b)** $\phi = 0.2$.

The consequences of vortex profiles acquired by the present study bear a similarity to the results attained via Majdalani [11]. Though, the existence of minor differences is virtue of the truth that Majdalani [11] pushed on a pulsatile drift in a rectangular duct. Figure 7(a)-7(d) indicates the influence of volume fraction ϕ on the radial profile of vorticity. According to the definition of vortex, it is a region in a fluid (both real and ideal) in which the flow is rotating around an axis line, which may be straight or curved. Mathematically it is obtained by operating the curl of velocity field and most of the cases this distribution/velocity of fluid is greater but symmetric along its axis. Results presented in Fig. 7 shows the resemblance according to the definition of vortex and it is noted that the magnitude of the vortices is higher at extreme position of the domain. Further it is noticed that distribution of vortex is getting squeeze with increasing values

of nanoparticle volume fraction ϕ (See Figures. 7(b)-7(d)). It is also notice that the vorticity takes negative values for certain phases for different ϕ values indicating the presence of a return flow. In comparison of Fig. 7(a)-7(d), obtained variation in vortex is very high for base fluid (ϕ = 0) as compare to the non-zero values of nanoparticle volume fraction.

The reduction of flow area ends in grows the velocity as its miles proven in figures 8(a)-8(d), where the velocity decreases with increase of nanoparticle volume fraction ϕ. In figure 8(a)-8(d), it is noticed that flow area construct set of envelop for various values of radius and velocity field attained maximum position with respect to increasing values of the radius. Since, internal radius of the cylinder remains less or equal to the radius of external cylinder so domain of the velocity profile restrict from $0 \leq r \leq 1$ so it may be visible that the velocity maximums are in the neighborhood of the conduits for the flow areas that change from 0.7 to 1 and the decline in the flow area result in lessen the annular effect.

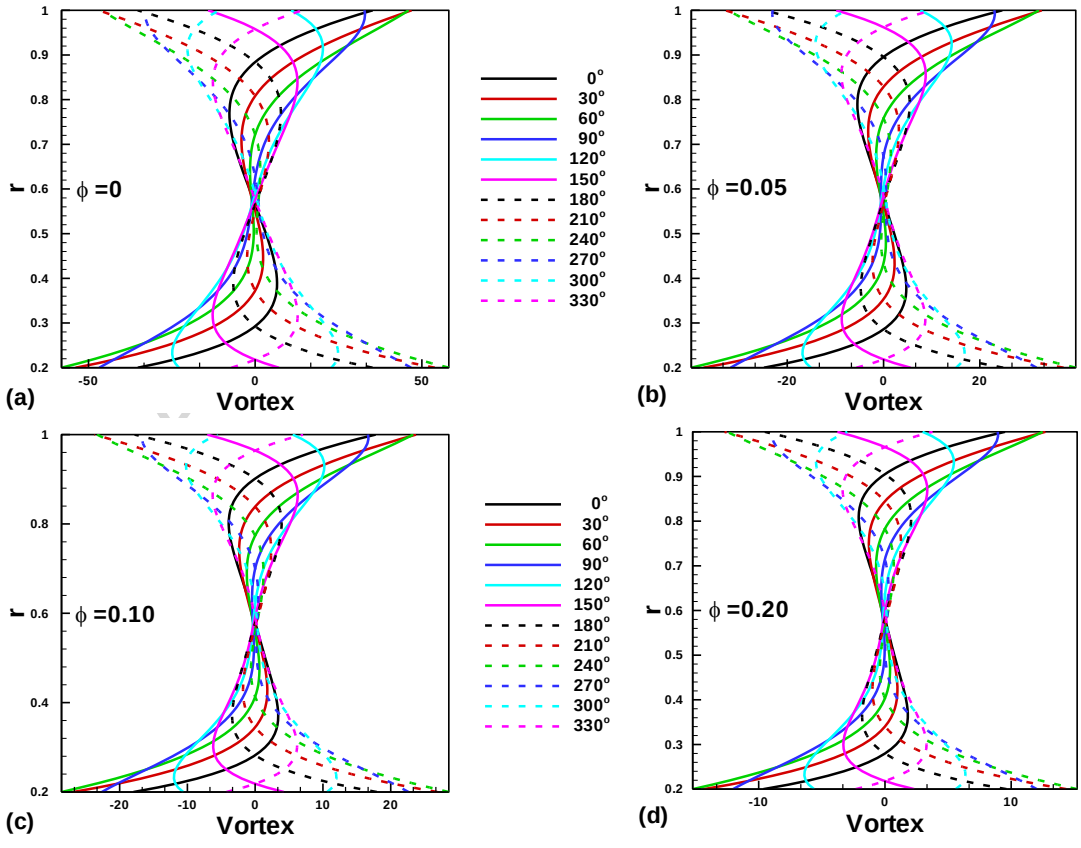

Fig. 7: Variation of vortex profile t for **(a)** ϕ = 0, **(b)** ϕ = 0.05, **(c)** ϕ = 0.1 **(d)** ϕ = 0.2 when $Re_\omega = 10, M = 5$.

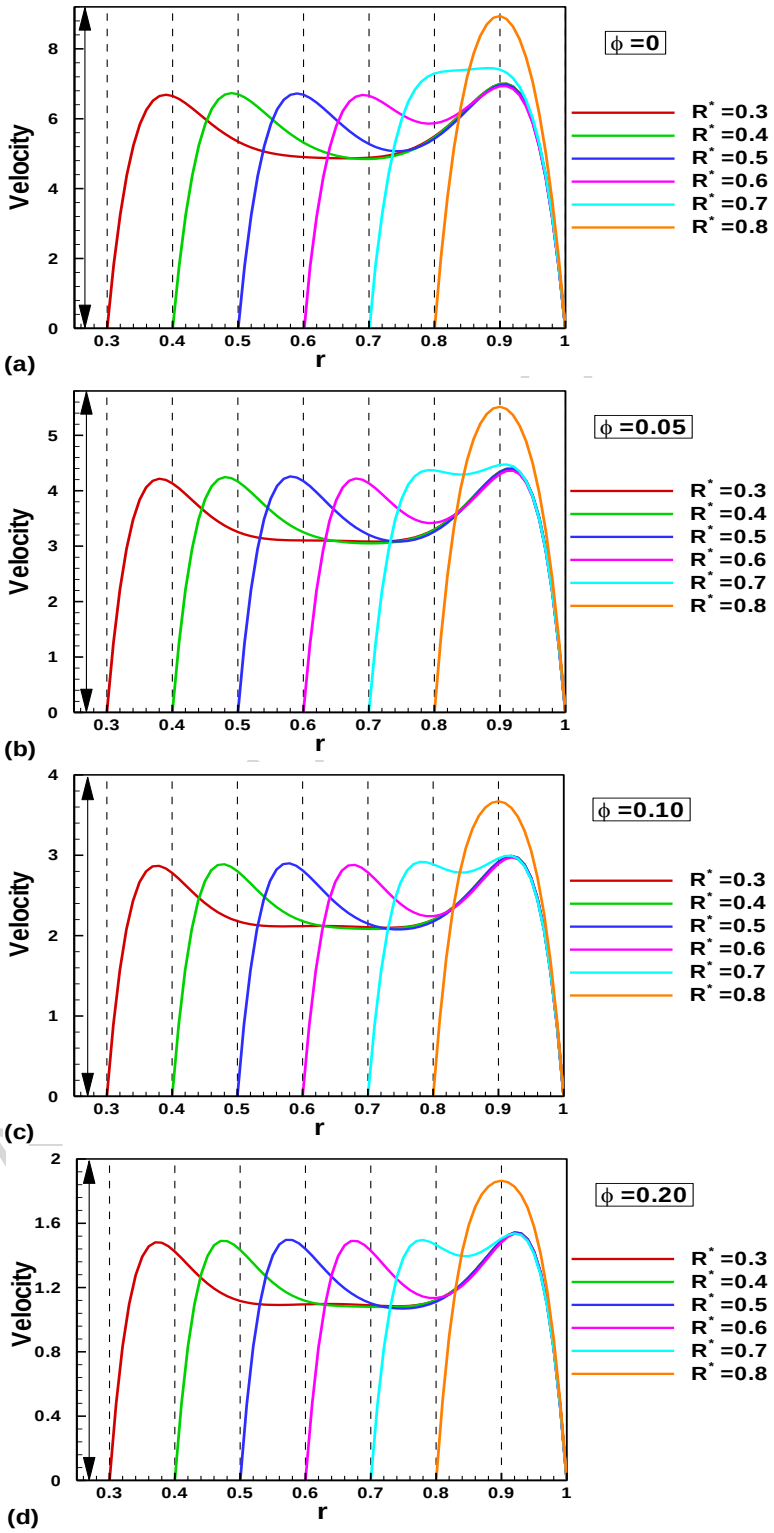

Fig. 8: Variation of velocity profile for various values of R^* **(a)** $\phi = 0$ **(b)** $\phi = 0.05$ **(c)** $\phi = 0.1$ **(d)** $\phi = 0.2$.

Exploration of heat transferal revolves around the study of temperature profile as well as heat transfer rate situated near the surface of the cylinder. To deal the influence of parameter at the temperature distribution results are plotted for nanoparticle volume fraction, Kinetic Reynolds number, amplitude of pressure gradient, Hartmann number, Prandtl number. In Figs. 9(a)-9(d), we have plotted the amplitude of pressure gradient at various position of R^*. It is found that when $R^* = 0.1$ then temperature profile reduces within the whole domain of the two ducts with increasing values of amplitude pressure gradient. However temperature profile switch its behavior from increasing to decreasing behavior for various values of amplitude pressure gradient at $R^* = 0.3, 0.5$. It is important to note that temperature profile switches twice its behavior at $R^* = 0.7$. Figure 10(a) shows the variation of dimensionless temperature profile for water-based *Cu* nanoparticles for varied volume fraction ϕ . It is spotted that with an increase of nanoparticles enhance the heat transfer profile. Based upon effective thermal conductivity it is further determined that water based *Cu* nanoparticles have higher heat transfer rate as compare to the base fluid (water) .Similarly Fig. 10(b) depicts the variation of temperature profile is plotted against Hartmann number M. One can observe that fluid temperature rises due to imposition of the transverse magnetic field. Since magnetic field produces the electric current in fluid which produces heat in the fluid, so the magnetic field with radiation assists the enhancement phenomena. Fig. 10(c) and 10(d) shows the effect of time on temperature profile. It is found that increase of time t rise the temperature profile.

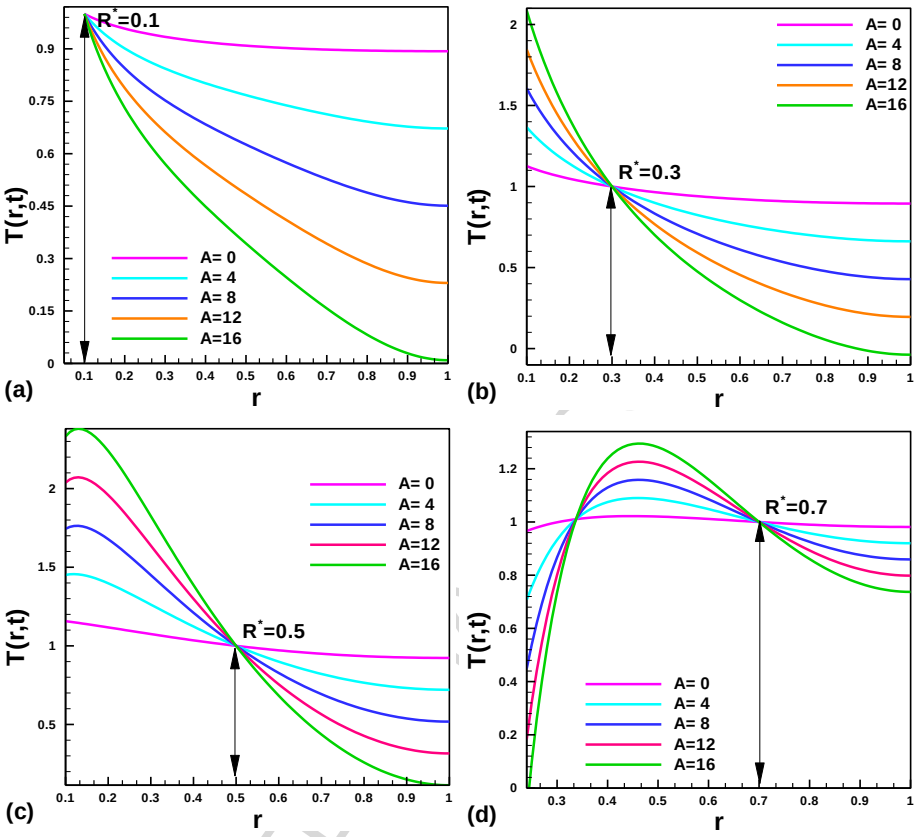

Fig. 9: Variation of temperature profile for various values of pressure gradient A when **(a)** $R^* = 0.1$ **(b)** $R^* = 0.3$ **(c)** $R^* = 0.5$ and **(d)** $R^* = 0.7$.

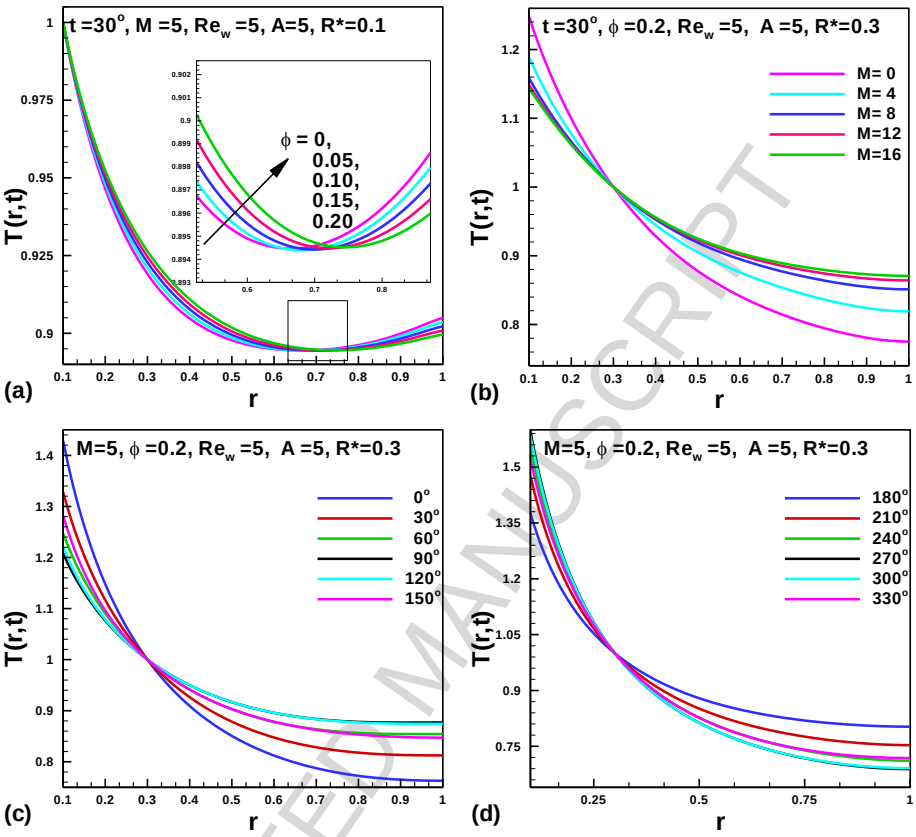

Fig.10. Variation of temperature profile for various values of **(a)** nanoparticles ϕ **(b)** Hartmann number M and **(c)** $0^{\circ} < t < 150^{\circ}$ **(d)** $180^{\circ} < t < 330^{\circ}$.

In Fig. 11, results are plotted for stream line to analyze the variation of flow behavior for base fluid and water based Cu nanoparticles. One can observe that these stream lines variate its pattern with respect to nanoparticle volume fraction ϕ. It is found that less numbers of contour are obtained in the absence of nanoparticles $\phi = 0$, while these contours takes the wider shape with respect to increase of nanoparticle volume fraction. Fig. 12 demonstrates the variation of pressure gradient for increasing values of nanoparticle volume fraction. It is found that, at the mean position of the duct with $t = 180^{\circ}$ pressure gradient is maximum but attained the decreasing behavior. However at $t = 0^{\circ}$ and $t = 360^{\circ}$ pressure gradient is minimum but predicts the increasing behavior by improving the values of ϕ. It is further observed that for $R^* = 0.1$, there is a maximum change in the pressure gradient as compare to the large value of $R^* = 0.3$.

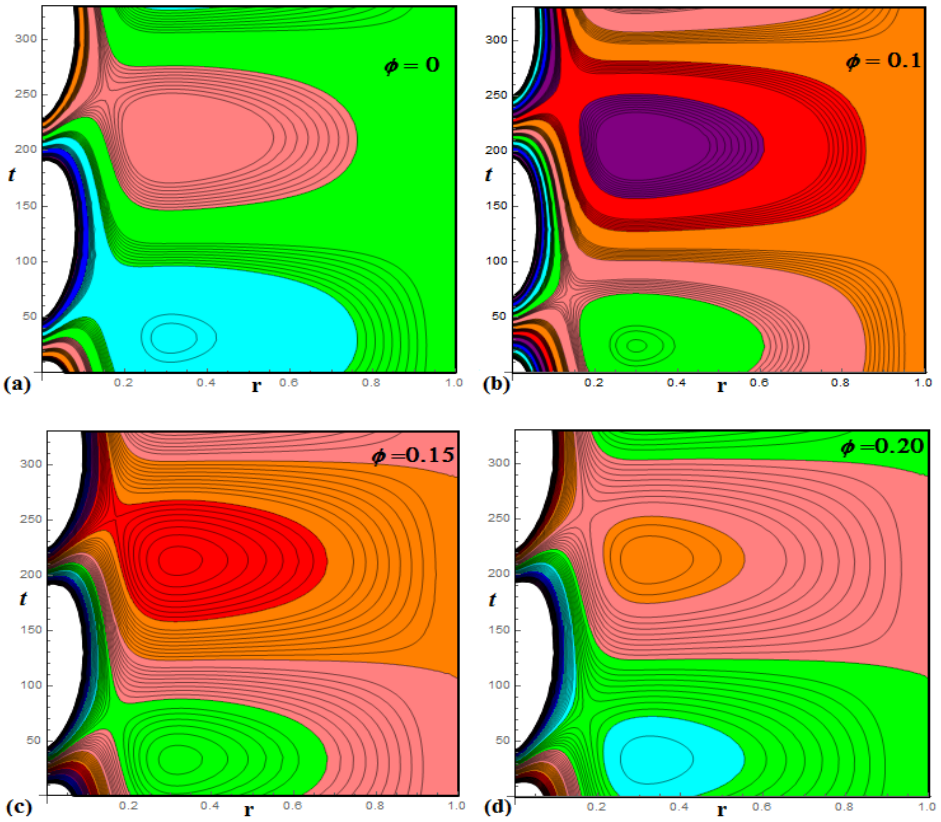

Fig. 11: Streamlines for water- based Cu nanoparticles for **(a)** base fluid (ϕ = 0) **(b)** ϕ = 0.05 **(c)** ϕ = 0.1 and **(d)** ϕ = 0.2.

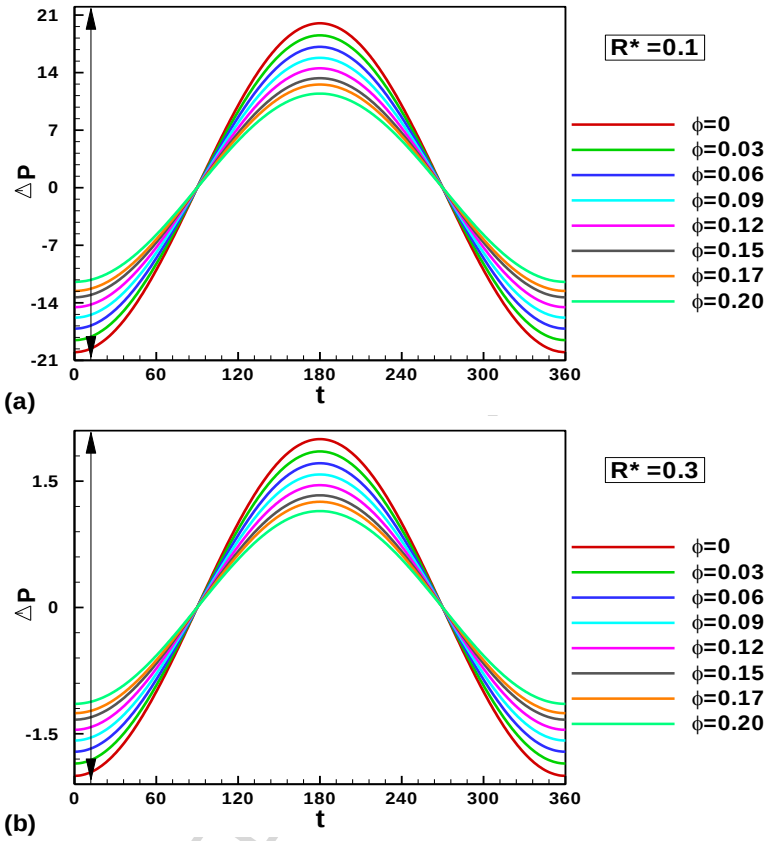

Fig. 12: Pressure gradient for **(a)** $R^* = 0.1$ and **(b)** $R^* = 0.3$, when $\bar{A} = 20, M = 10, \alpha = 10$.

5. Conclusions

We have discussed the MHD pulsatile flow of nanofluid between two concentric ducts. Exact solutions for velocity, pressure and temperature distribution in case of a pulsatile flow for nanofluid is obtained between two ducts. The consequence of magnetic field on heat transfer has been studied analytically, which is valuable for the knowledge of blood behavior when exposed to a magnetic field. It can be concluded that the flow of blood and pressure can be controlled sufficiently by the application of an external magnetic field. This will help to reduce some arterial diseases. The solutions for the velocity, pressure and temperature are shown graphically for a wide range of Reynolds numbers, volume fractions, Prandtl numbers and Hartmann numbers. Moreover, the results confirmed that the velocity and temperature may be controlled with the aid of the outside magnetic field and so the heat transfer can be decreased or improved by grasping the amount of the magnetic field. Amplitude of velocity decreases by improving the

values of ϕ. It is further analyzed that addition of copper nanoparticles rising the temperature of water.

Acknowledgment

Authors would like to acknowledge and express their gratitude to the United Arab Emirates University, Al Ain, UAE for providing the financial support with Grant No. 31S212-UPAR (9) 2015.

6. References

[1] Atabek H.B. and Chang C C. Oscillatory flow near the entry of circular tube, zamp. Vol. 12, P.405422. 1961.

[2] Vardanyan VA Effect of magnetic field on blood flow. Biofizika, 18(3). 491-496 .1973.

[3] P. Chaturani, V. Palanisamy, Pulsatile flow of blood with periodic body acceleration, International Journal of Engineering Science, 29(1) (1991) 113-121.

[4] Moustafa El-Shahed , Pulsatile flow of blood through a stenosed porous medium under periodic body acceleration, Applied Mathematics and Computation 138 (2003) 479–488.

[5] Pankaj Mathur, Surekha Jain, Pulsatile flow of blood through a stenosed tube: effect of periodic body acceleration and a magnetic field, Journal of Biorheology, 25(1) (2011) 71-77.

[6] D.S. Sankar, K. Hemalatha, Pulsatile flow of Herschel–Bulkley fluid through catheterized arteries–A mathematical model, Applied Mathematical Modelling, 31(8) (2007) 1497-1517.

[7] D. C. Sanyal and A. Biswas, ―pulsatile motion through an axisymmetric artery in presence of magnetic field, Assam University Journal of Science & Technology.Physical Science and Technology, vol. 5, no. 2, pp. 12-20, 2010.

[8] Yakhot A, Grinberg L. Phase shift ellipses for pulsating flows Physics of Fluids. Vol 15, Number 7.July2003.

[9] Suces J. An improved quasi-study approach for transient conjugated forced convection problems. Int.J. Heat. Mass.Trans. Vol.24, n0 10, pp1711-1722, 1981.

[10] T. W. Latham, Fluid motions in a peristaltic pump, M.Sc. Thesis. 1. Massachusetts Institute of Technology, Cambridge, 1966.

[11] Majdalani. Pulsatory channel flows with arbitrary pressure gradients.AIAA.3rd.Theoretical fluid mechanics meeting. 24-26. June 2002.

[12] Agrawal HL, Anwaruddin B. Peristalic flow of blood in a branch. Ranchi Univ Math J, 1984, 15:111-121.

[13] E. E. Tzirtzilakis, A Mathematical Model for Blood Flow in Magnetic Field,Physics of Fluids, vol. 17, no. 7, 2005, p. 077103, 2005.

[14] G. Ramamurthy and B. Shanker, Magneto hydrodynamic Effects on Blood Flow through Porous Channel, Medical and Biological Engineering and Computing, vol. 32, no. 6, pp. 655-659, 1994.

[15] Choi, S. U .S. Enhancing Thermal Conductivity of fluids with Nanoparticles, in: D. A. Siginer, H.P. Wang (Eds.), Developments and Applications of Non-Newtonian Flows, ASME FED, 1995, 231, 99-103.

[16] Choi, S. U .S. Nanofluids from vision to reality through research, J. of Heat Transfer, 2009, 131, 1-9.

[17] Yu, W.; France, D. M.; Routbort, J. L. and Choi., S. U. S. Reviewand comparison of nanofluid thermal conductivity and heat transfer enhancements, Heat Transfer Eng., 2008, 29, 432-460.

[18] Das, S. K.; Choi, S. U. S. and Patel., H. E.; Heat transfer in nanofluids-A review, Heat Transfer Eng., 2006, 27, 3-9.

[19] Liu, M. S.; Lin, M. C. C.; Huang, I. T. and Wang, C. C. Enhancement of thermal conductivity with carbon nanotube for nanofluids, Int. Commun. in Heat and Mass Transfer, 2005, 32, 1202-1210.

[20] Buongiorno., J. Convective Transport in Nanofluids, J. of Heat Transfer. 2005, 128, 240-250.

[21] Akbar, N. S. and Nadeem, S. Mixed convective Magnetohydrodynamic peristaltic flow of a Jeffrey nanofluid with Newtonian heating, Zeitschrift fur Naturforschung A., 2013, 68, 433-441.

[22] Emad, A. H., Ebaid, A. New exact solutions for boundary-layer flow of a nanofluid past a stretching sheet, J. Comput. and Theor.Nanosci., 2013, 10, 2591-2594.

[23] Ebaid, A. and Wazwaz, A. M. On the generalized Exp-function method and its application to boundary layer flow at nano-scale, J. Comput. Theor. Nanosci., 2014, 11,178-184.

[24] Rizwan Ul Haq, S.T. Hussain, Z.H. Khan, Z. Hammouch, Flow and Heat transfer analysis of Water and Ethylene Glycol based Cu nanoparticles between two parallel disks with Suction/Injection effects, J. Mol. Liq., 221 (2016) 298–304.

[25] Sajjad-ur Rehman, Rizwan-ul Haq, Zafar Hayat Khan, Changhoon Lee, Entropy generation analysis for non-Newtonian nanofluid with zero normal flux of nanoparticles at the stretching surface, Journal of the Taiwan Institute of Chemical Engineers, 63, (2016) 226-235

[26] S.T. Hussain, Rizwan-ul- Haq, Z.H. Khan, S. Nadeem, Water driven flow of carbon nanotubes in a rotating channel, Journal of Molecular Liquids, 214 (2016), 136-144.

[27] S. Saleem, S. Nadeem, Rizwan Ul Haq, Buoyancy and metallic particle effects on an unsteady water-based fluid flow along a vertically rotating cone, The European Physical Journal Plus, 129 (2014) 213.

[28] Rizwan Ul Haq, Sohail Nadeem, Z.H. Khan, N.F.M. Noor, Convective heat transfer in MHD slip flow over a stretching surface in the presence of carbon nanotubes, Physica B: Condensed Matter, 457(15) (2015) 40-47.

[29] Rizwan Ul Haq, Zakia Hammouch, Waqar Ahmed Khan, Water-based Squeezing Flow in the presence of Carbon Nanotubes between Two Parallel Disks. Thermal Science. Doi: 10.2298/TSCI141102148H.

[30] Wubshet Ibrahim, Rizwan Ul Haq, Magnetohydrodynamic (MHD) stagnation point flow of nanofluid past a stretching sheet with convective boundary condition, Journal of the Brazilian Society of Mechanical Sciences and Engineering, DOI 10.1007/s40430-015-0347-z. (2015).

[31] W. A. Khan, R Culham, Rizwan Ul Haq, Heat Transfer Analysis of MHD Water Functionalized Carbon Nanotube Flow over a Static/Moving Wedge, Journal of Nanomaterials, Volume 2015 (2015), Article ID 934367, 13, doi.org/10.1155/2015/934367.

[32] W.A. Khan, Z.H. Khan, Rizwan Ul Haq, Flow and heat transfer of ferrofluids over a flat plate with uniform heat flux, The European Physical Journal Plus, (130) 86 (2015).

[33] Rizwan Ul Haq, S. Nadeem, Z. H. Khan, N.F.M. Noor, MHD squeezed flow of water functionalized metallic nanoparticles over a sensor surface, Physica E: Low-dimensional Systems and Nanostructures, (73) (2015) 45-53.

[34] S. T. Hussain, Rizwan Ul Haq, Z. H. Khan, S. Nadeem, Water Driven Flow of Carbon nanofluid nanotubes in a rotating channel, Journal of Molecular Liquid, 214 (2016) 136-144.

[35] S. T. Hussain, S. Nadeem, Rizwan Ul Haq, Model based analysis of micropolar nanofluid flow over a stretching surface, The European Physical Journal Plus, 129:167 (2014).

[36] Rizwan Ul Haq, S. Nadeem, Z. H. Khan, O. T. Gideon, Convective Heat Transfer and MHD Effects on Casson Nanofluid Flow over a Shrinking Sheet, Central European Journal of Physics, 12(12), (2014) 862-871.

[37] S.K. Mohammadian, S.M. Rassoulinejad-Mousavi, Y. Zhang, Thermal management improvement of an air–cooled high-power lithium-ion battery by embedding metal foam, J. Power. Sources 296 (2015) 305-313.

[38] S.M. Rassoulinejad-Mousavi, H. Yaghoobi, Effect of non-linear drag term on viscous dissipation in a fluid saturated porous medium channel with various boundary conditions at walls, Arab. J. Sci. Eng. 39 (2) (2014) 1231–1240.

[39] A. Shirazpour, S.M. Rassoulinejad-Mousavi, and H.R. Seyf, (2011) HPM Solution of Momentum Equation for Darcy-Brinkman Model in Parallel Plates Channel Subjected to Lorentz Force. International Journal of Mechanical, Aerospaces, Mechatronic and Manufacturing Engineering, 5, 258-262.

[40] R. L. Hamilton, O. K. Crosser, Thermal conductivity of heterogeneous two-component systems. Ind. Eng. Chem. Fund., 1(3) (1962) 187–191.

Graphical Abstract:

Analysis is performed for Cu–water nanofluid with oscillating pressure gradient between two concentric cylinders. These important results are shows the important effects of vortex profile and flow area on the velocity profile.

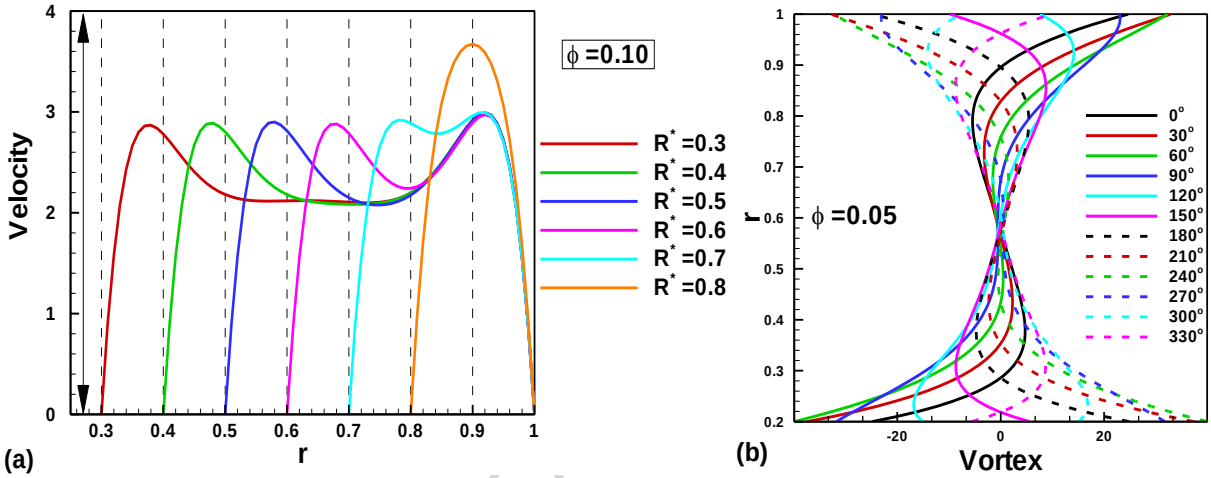

Research Highlights:

- Analysis is performed for MHD nanofluid between two concentric cylinders.
- Attained results depict the dominant enhancement in the thermal conductivity of base fluid.
- Oscillatory pressure gradient is applied to provide the interrupt within the nanofluid.
- An efficient and dominant effect can be analyze for vortex profile and flow area on the velocity profile.